Electronic Supporting Information

For

Efficiently Reducing the Plant Growth Inhibition of CuO NPs by Rice Husk Derived Biochar: Experimental Demonstration and Mechanism Investigation

Xiao-Feng Sima,[a] Xian-Cheng Shen,[a] Tao Fang,[b] Han-Qing Yu[a] and Hong Jiang[a]*

[a] CAS Key Laboratory of Urban Pollutant Conversion, Department of Chemistry, University of Science & Technology of China, Hefei, 230026, P.R. China

[b] Institute of Hydrobiology, Chinese Academy of Sciences, Wuhan, 430072, P.R. China

*** Corresponding author:**

Dr. Hong Jiang

Fax: 86-551-63607482; E-mail: jhong@ustc.edu.cn

Content

Text S1

Seed Germination. Wheat seeds were surface sterilized with 10% H_2O_2 solution for 10 min and then rinsed three times with deionized water. The seeds were then immersed in deionized water or NPs suspension (10, 50, 100, 500 mg L^{-1}) for 2h. 5 mL CuO NPs suspensions with each concentration and 3% biochar (w/v) were added into 90 mm diameter × 15 mm depth Petri dishes lined with a filter paper. The seeds were subsequently placed in each dish (20 seeds each). The germination experiments were performed in five replicates, and control experiment was also conducted in the same suspension without biochar. The seeds were germinated in the dark by wrapping the Petri dishes with aluminum foil, and placed in a growth chamber with 14-h photoperiod, day/night temperature of 25/20 °C, and 65% relative humidity. Germination was quantified when the bud length surpassed half of the seed length. In addition, the length of roots and shoots were measured over the course of 4 d.

Table S1. Characteristics of CuO nanoparticles used in this study.

Table S2. Physicochemical characteristics of biochar used in this study.

Table S3. The functional group of pristine biochar and biochar with Cu^{2+} adsorption determined by FTIR.

Figure S1. Transmission electron micrograph of CuO nanoparticle suspensions.

Figure S2. Frequency of size distribution of CuO NPs in nutrient solution determined by DLS.

Figure S3. SEM micrographs of the surface of the bio-chars.

Figure S4. The germination rate after 4 d germination in various concentrations CuO NPs suspension with and without biochar. Treatments resulting in significant difference are indicated by different letters ($p<0.05$).

Figure S5. Ratio of root and shoot elongation with biochar to those without biochar after 4 d germination.

Figure S6. The ratio of the roots and shoots growth length with biochar to those without biochar after 9d in hydroponic culture experiment.

Figure S7. The ratio of weight of tissue with biochar to those without biochar in hydroponic culture experiment.

Figure S8. The length growth of roots (A) and shoots (B) in continuous hydroponic culture experiment of various concentrations CuO NPs suspension with and without biochar. Treatments resulting in significant difference are indicated by different letters ($p<0.05$).

Figure S9. The length growth of roots (A) and shoots (B) in hydroponic culture experiment of various concentrations Cu^{2+} solution. Treatments resulting in significant difference are indicated by different letters ($p<0.05$).

Figure S10. (A) The concentration of Cu^{2+} released from different suspensions (100 mg L^{-1} CuO NPs, 100 mg L^{-1} CuO NPs + plant, 100 mg L^{-1} CuO NPs + biochar, 100 mg L^{-1} CuO NPs + plant + biochar). (B) Adsorption kinetics of Cu^{2+} on biochar.

Figure S11. The time dependent adsorption of Cu^{2+} by biochar (initial Cu^{2+} concentration: 200 mg L^{-1}; adsorption dosage: 30 g L^{-1}).

Figure S12. FTIR spectra of pristine biochar and biochar with Cu^{2+} adsorption.

Figure S13. XRD patterns of biochar with Cu^{2+} adsorption.

Figure S14. SEM images of wheat root surface in hydroponic culture experiment under treatment of (a) 100 mg L^{-1} CuO NPs, and (b) 100 mg L^{-1} CuO NPs + biochar. Representative EDS analysis of the selected area in SEM pictures (c) and (d).

Table S1. Characteristics of CuO nanoparticles used in this study.

Particle		CuO NPs
Particle size by TEM (nm)		15.7 ± 5.8
Purity (%)		＞ 99.9%
Surface area (m^2 g^{-1})		13.1
In 25% strength Hoagland solution	pH	6.49
	Conductivity (μs cm^{-1})	901 ± 12
	Zeta potential (mV)	-12.6 ± 1.2
	Hydrodynamic size by DLS (nm)	350 ± 28

Table S2. Physicochemical characteristics of biochar used in this study.

Surface area (m^2/g)	Pore volume (cm^3/g)	Pore size (nm)	Elemental compositions (wt. %)				Ash (wt. %)
			C	H	O	N	
78.6	0.051	2.6	32.8	2.2	13.7	0.35	51.5

Table S3. The functional group of pristine biochar and biochar with Cu^{2+} adsorption determined by FTIR.

Functional group	Band positions (cm^{-1})	
	Pristine biochar	Biochar with
O-H stretch	3435	3440
Aliphatic C–H stretch	2923	2923
	2854	2854
Aromatic C–C stretch	1618	1619
C–O stretch	1384	1384
Si–O–Si asymmetric vibration	1101	1102

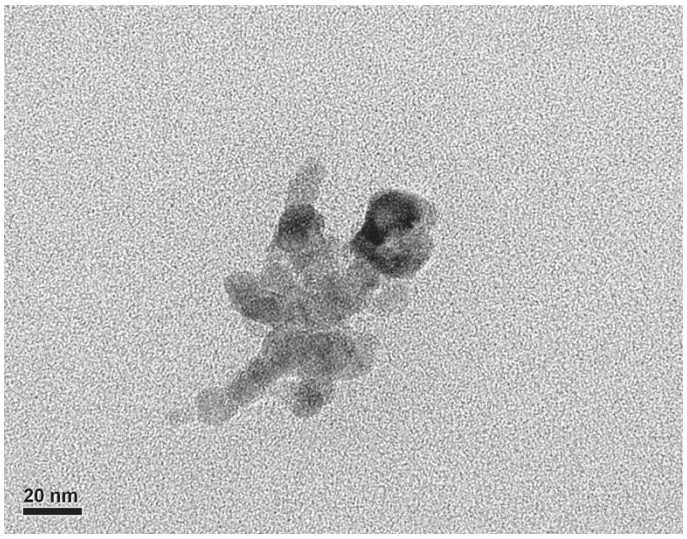

Figure S1. Transmission electron micrograph of CuO nanoparticle suspensions.

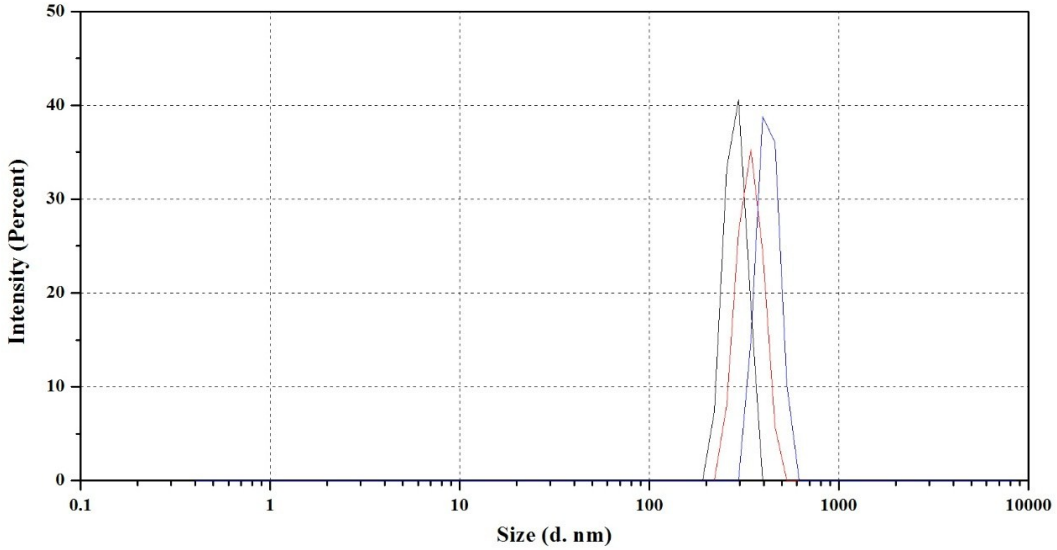

Figure S2. Frequency of size distribution of CuO NPs in nutrient solution determined by DLS.

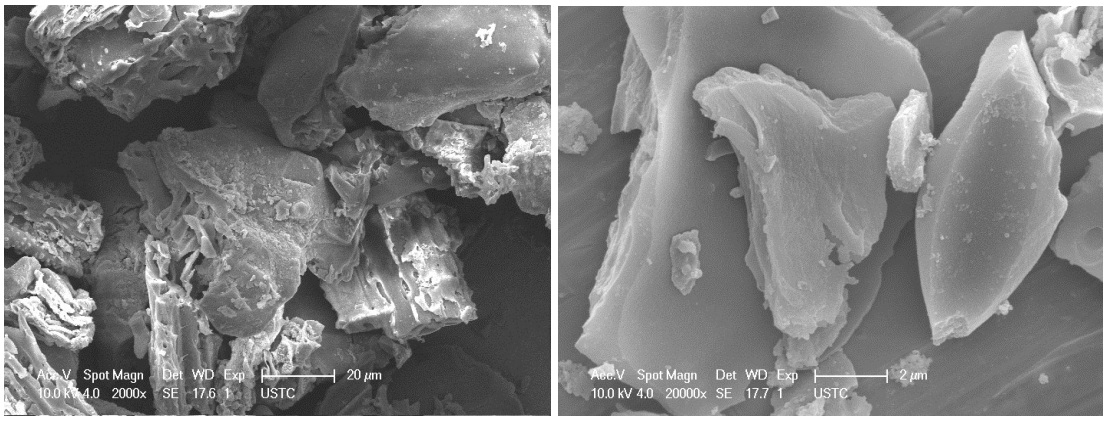

Figure S3. SEM micrographs of the surface of the bio-chars.

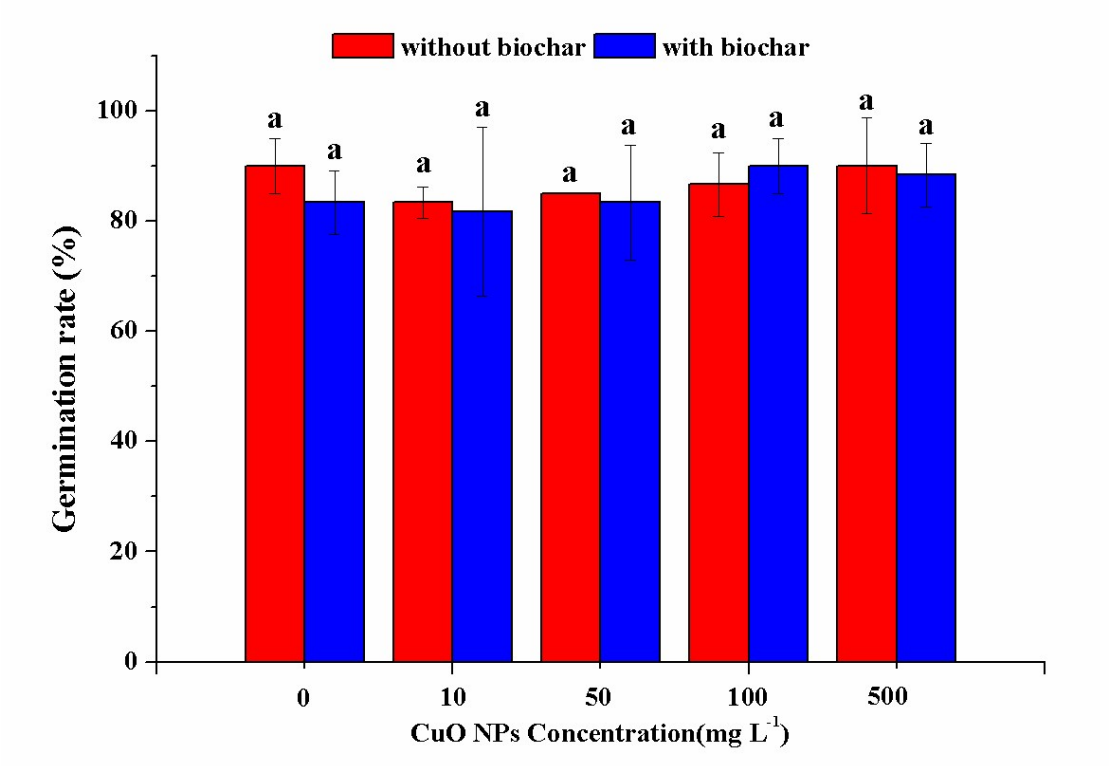

Figure S4. The germination rate after 4 d germination in various concentrations CuO NPs suspension with and without biochar. Treatments resulting in significant difference are indicated by different letters ($p<0.05$).

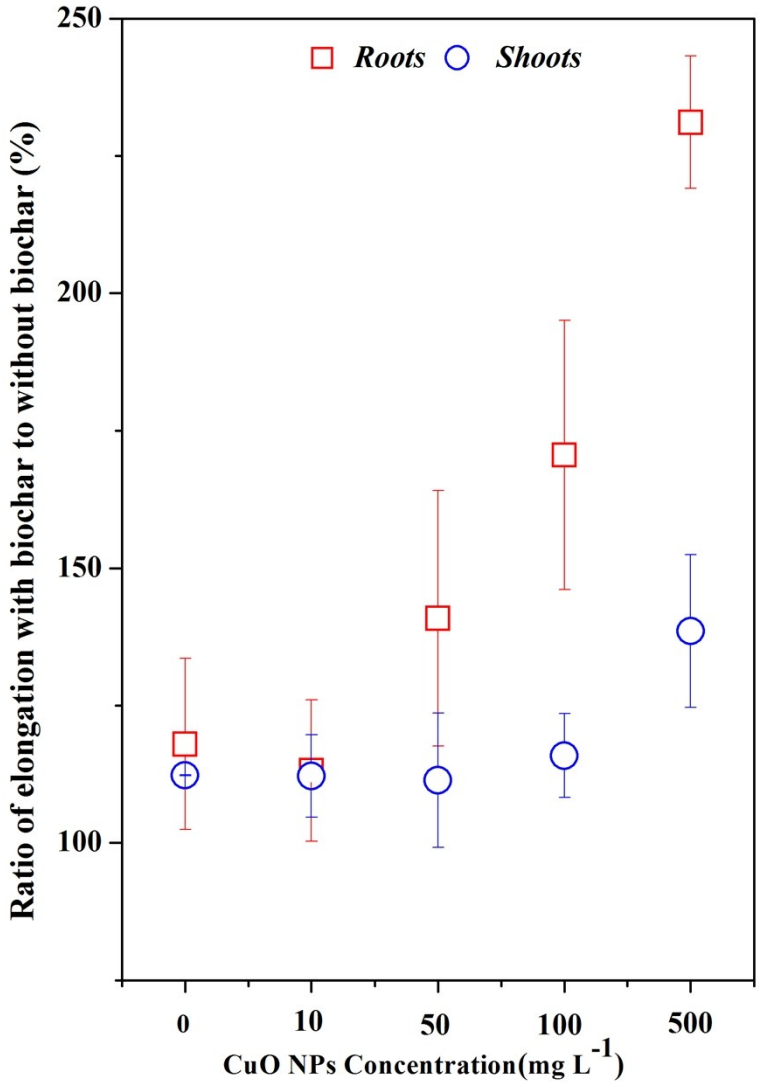

Figure S5. Ratio of root and shoot elongation with biochar to those without biochar after 4 d germination.

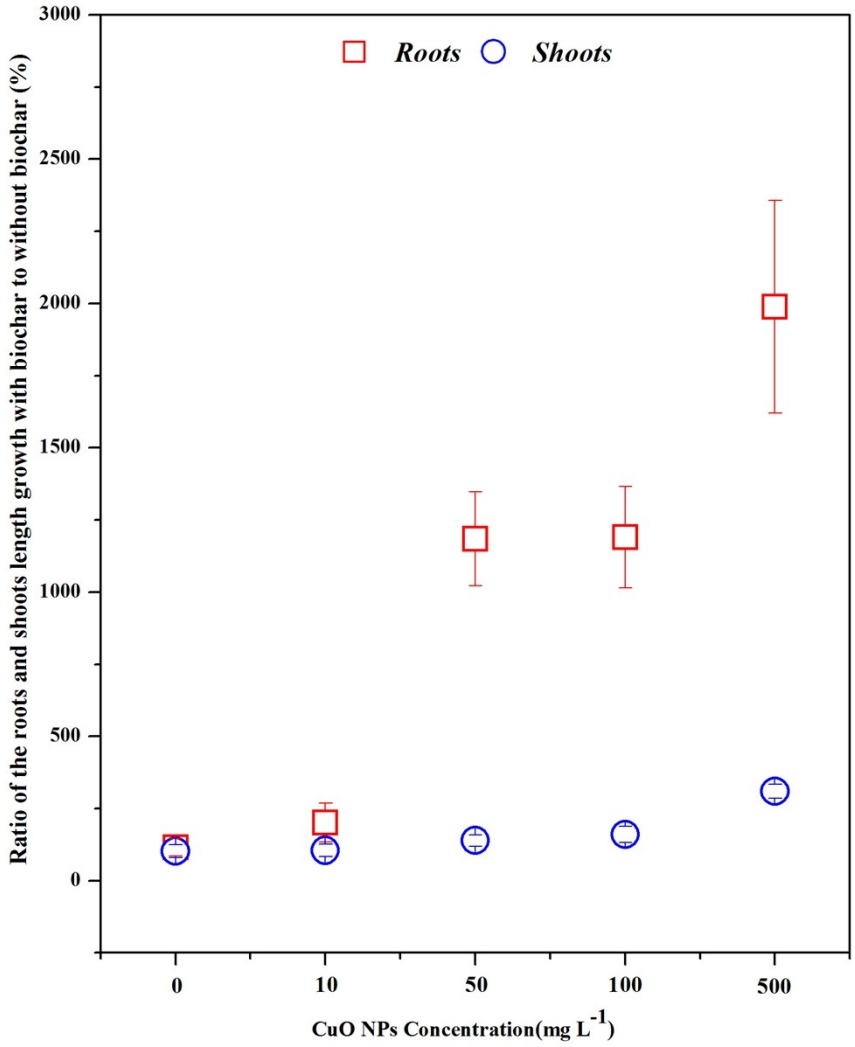

Figure S6. The ratio of the roots and shoots growth length with biochar to those without biochar after 9d in hydroponic culture experiment.

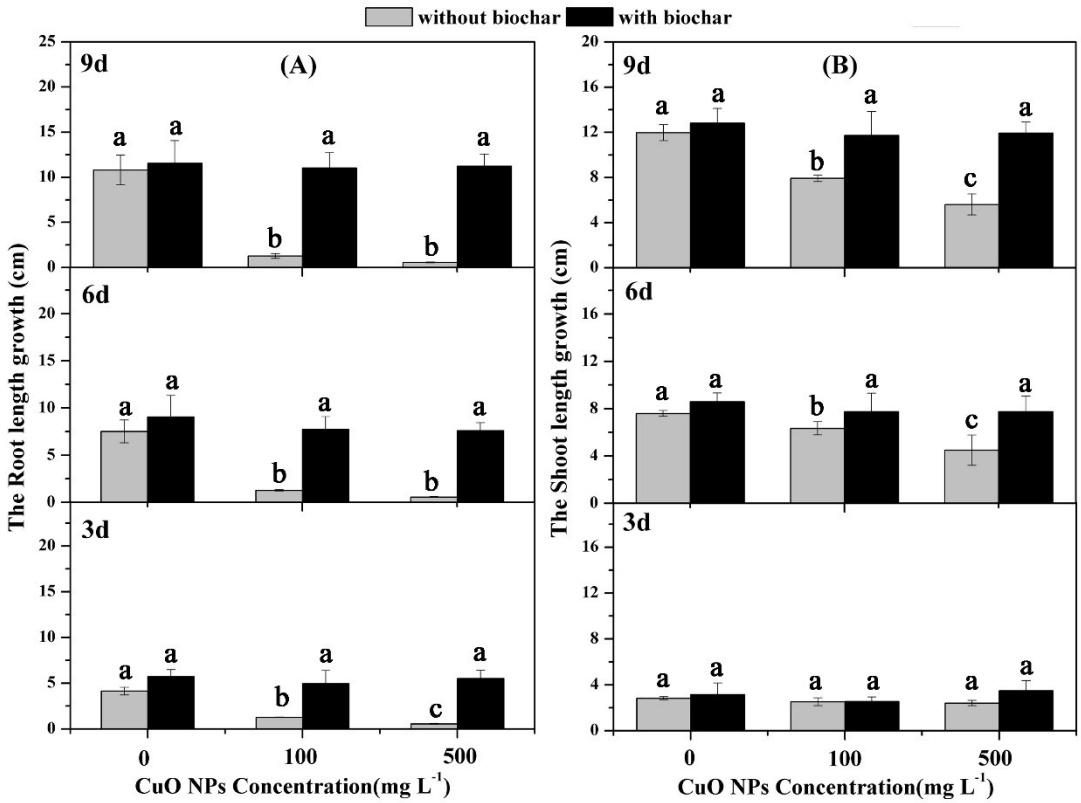

Figure S7. The length growth of roots (A) and shoots (B) in continuous hydroponic culture experiment of various concentrations CuO NPs suspension with and without biochar. Treatments resulting in significant difference are indicated by different letters ($p<0.05$).

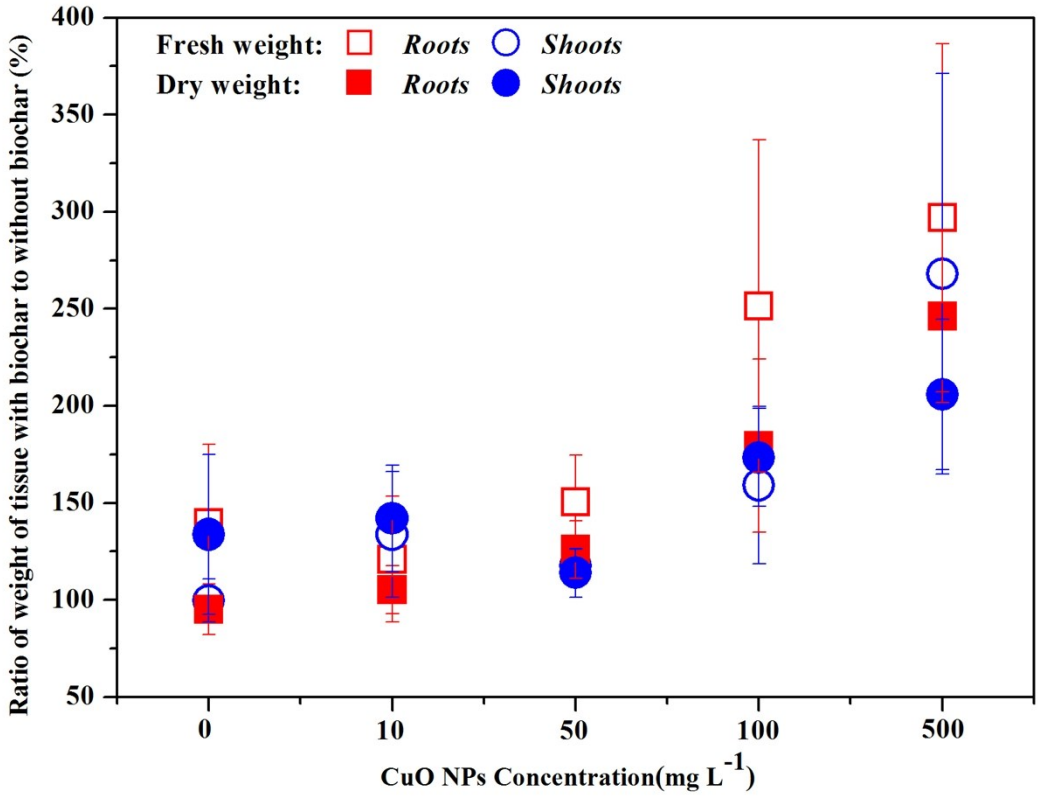

Figure S8. The ratio of weight of tissue with biochar to those without biochar in hydroponic culture experiment.

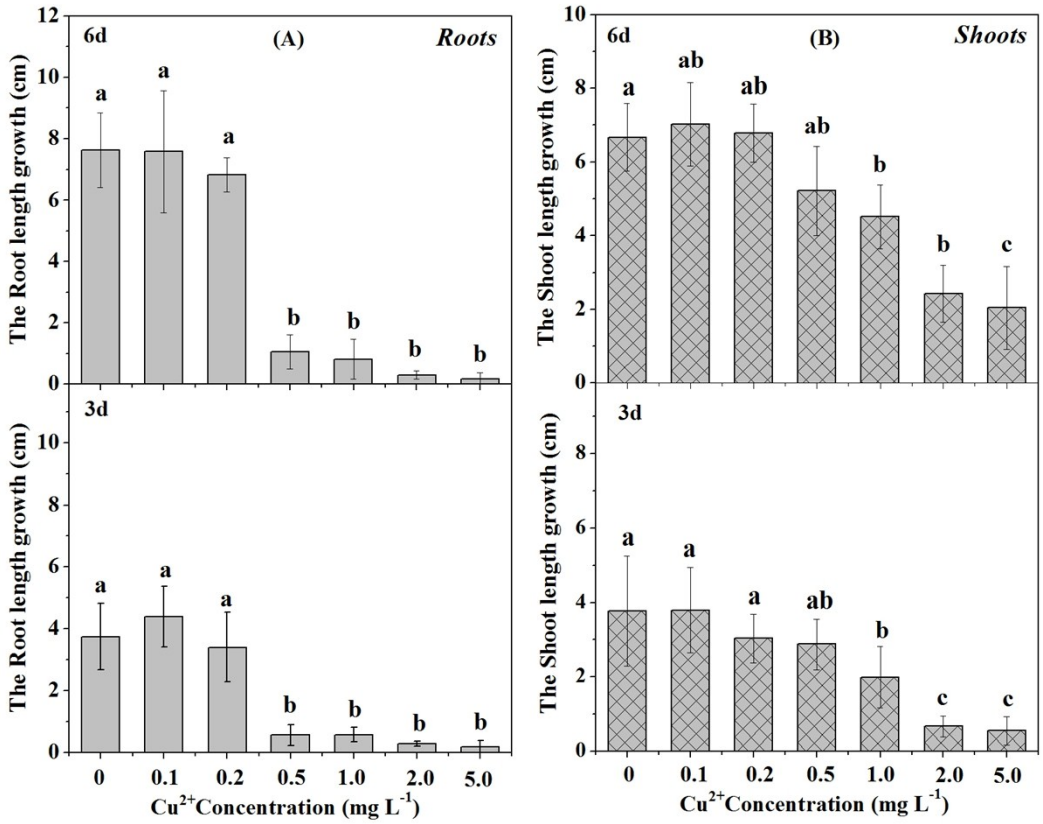

Figure S9. The length growth of roots (A) and shoots (B) in hydroponic culture experiment of various concentrations Cu^{2+} solution. Treatments resulting in significant difference are indicated by different letters ($p<0.05$).

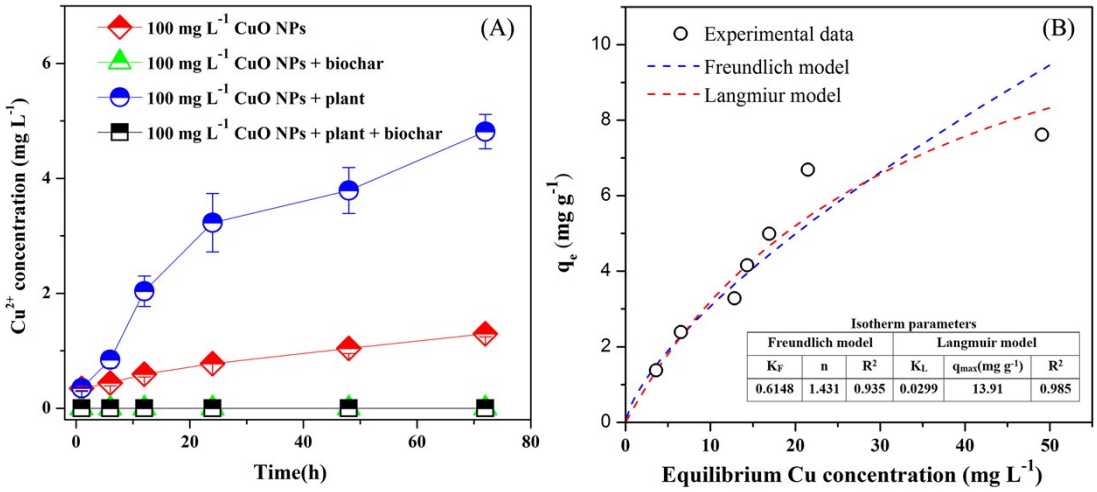

Figure S10. (A) The concentration of Cu^{2+} released from different suspensions (100 mg L^{-1} CuO NPs, 100 mg L^{-1} CuO NPs + plant, 100 mg L^{-1} CuO NPs + biochar, 100 mg L^{-1} CuO NPs + plant + biochar). (B)The adsorption isotherms of Cu^{2+} adsorption by biochar (dosage: 30 g L^{-1}; time: 3 d).

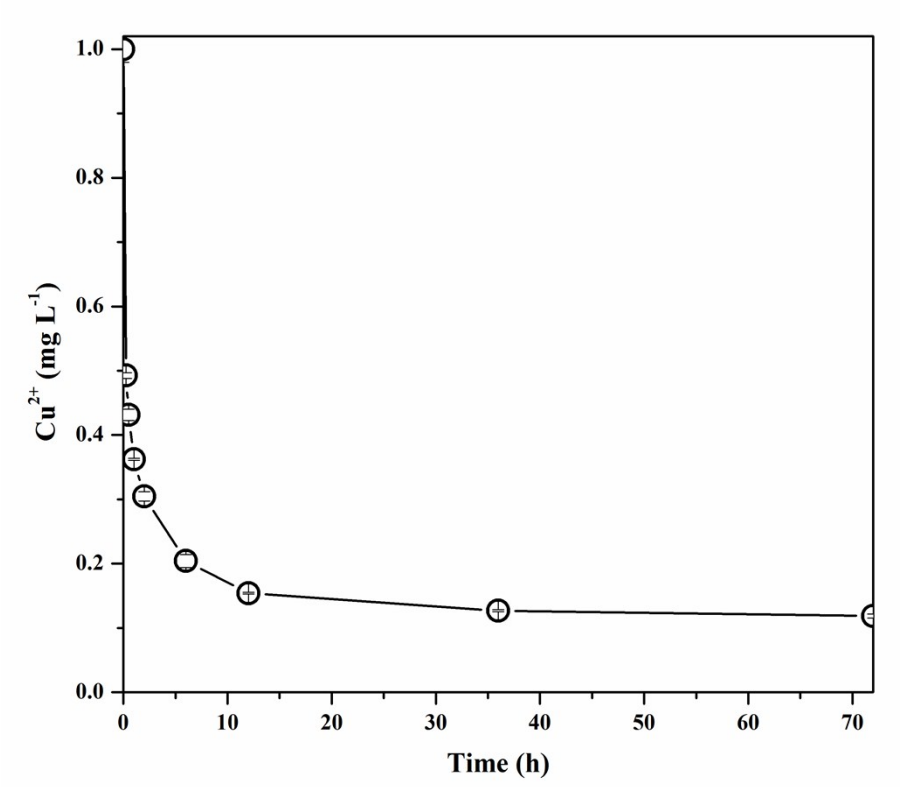

Figure S11. The time dependent adsorption of Cu^{2+} by biochar (initial Cu^{2+} concentration: 200 mg L^{-1}; adsorption dosage: 30 g L^{-1}).

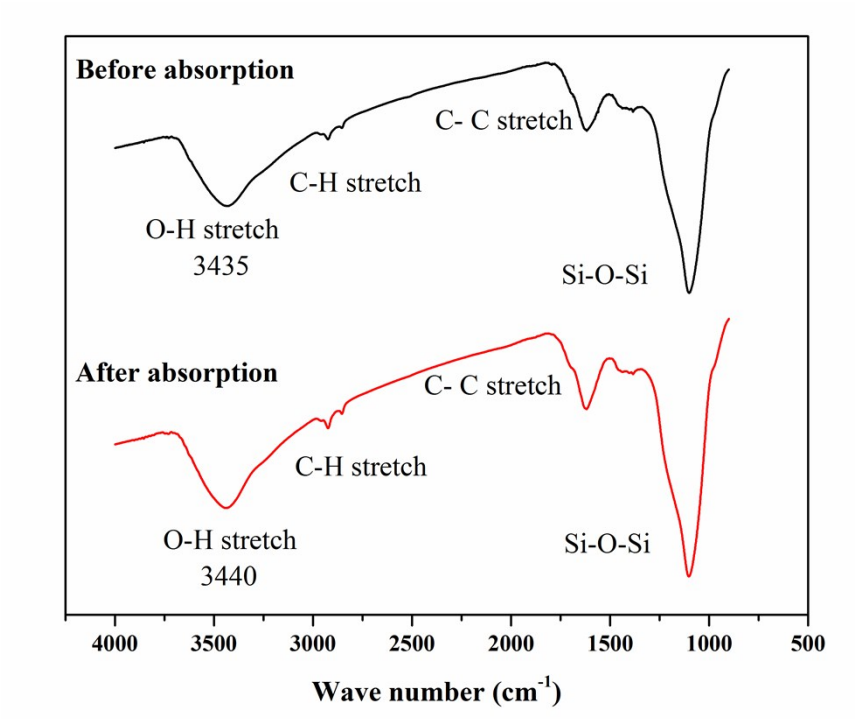

Figure S12. FTIR spectra of pristine biochar and biochar with Cu^{2+} adsorption.

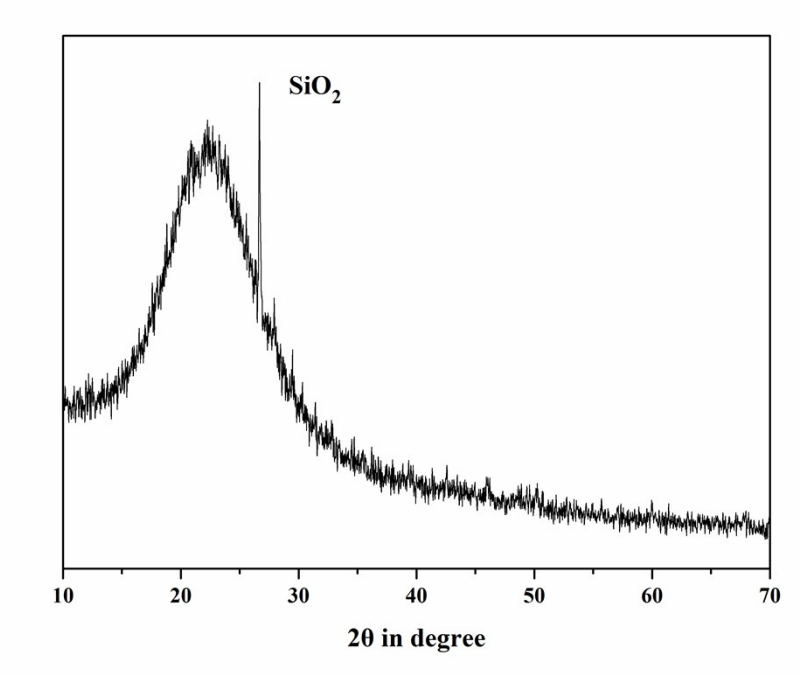

Figure S13. XRD patterns of biochar with Cu^{2+} adsorption.

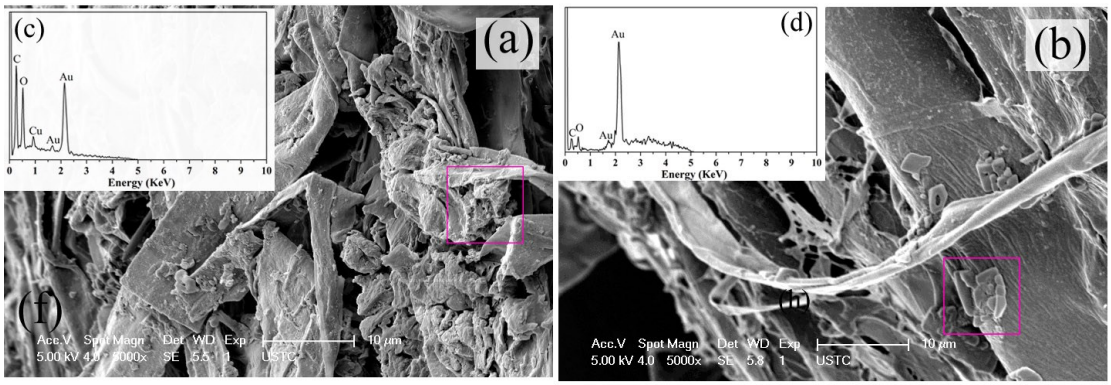

Figure S14. SEM images of wheat root surface in hydroponic culture experiment under treatment of (a) 100 mg L^{-1} CuO NPs, and (b) 100 mg L^{-1} CuO NPs + biochar. Representative EDS analysis of the selected area in SEM pictures (c) and (d).